

Supporting information for

Factors affecting chlorinated product formation from sodium hypochlorite bleach and limonene reactions in the gas phase

Callee M. Walsh*, Notashia N. Baughman, Jason E. Ham, J.R. Wells

Health Effects Laboratory Division, NIOSH, Morgantown, WV 26505

* To whom correspondence should be addressed: qqf2@cdc.gov

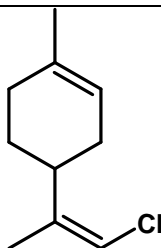
Table of Contents:

Table S1

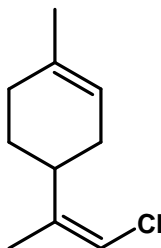
Figures S1-S19

Table S1. Detailed description of chlorinated products detected in gas-phase reactions between limonene and HOCl/Cl₂

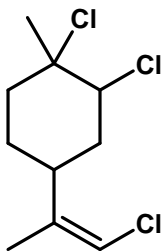
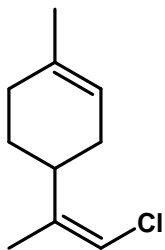
Structure ID	Structure	RT	Formula	Theoretical Monoisotopic (m/z)	Experimental Monoisotopic (m/z)	EI fragments observed (m/z)	Formula of fragments	ppb ¹	Yield (%)
4	 <chem>C=C(C)c1ccccc1C(Cl)(Cl)C</chem>	18.37	C ₁₀ H ₁₅ Cl ₃	240.0234	240.0238	205.0547 171.0749 169.0779 133.1013 119.0856 105.0700 91.0543	C ₁₀ H ₁₅ ³⁵ Cl ₂ C ₁₀ H ₁₄ ³⁷ Cl C ₁₀ H ₁₄ ³⁵ Cl C ₁₀ H ₁₃ C ₉ H ₁₁ C ₈ H ₉ C ₇ H ₇		
1	 <chem>C=C(C)c1ccccc1C(Cl)C</chem>	21.13	C ₁₀ H ₁₅ Cl	170.0857	170.0855	135.1167 127.0308 119.0855 91.0542 79.0542	C ₁₀ H ₁₅ C ₇ H ₈ ³⁵ Cl C ₉ H ₁₁ C ₇ H ₇ C ₆ H ₇		



1		21.59	$C_{10}H_{15}Cl$	170.0857	170.0854	135.1167 127.0308 119.0855 93.0699 91.0542 79.0542	$C_{10}H_{15}$ $C_7H_8^{35}Cl$ C_9H_{11} C_8H_9 C_7H_7 C_6H_7	46 ± 11	57 ± 8.7
---	--	-------	------------------	----------	----------	---	--	---------	----------



1		21.80	$C_{10}H_{15}Cl$	170.0857	170.0856	135.1168 134.1089 119.0855 105.0699 93.0699 91.0543 77.0386	$C_{10}H_{15}$ $C_{10}H_{14}$ C_9H_{11} C_8H_9 C_7H_9 C_7H_7 C_6H_5	
---	--	-------	------------------	----------	----------	---	---	--



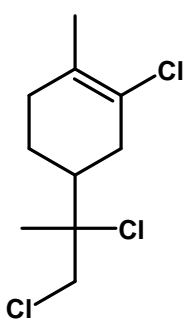
4

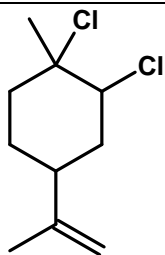
21.96 $C_{10}H_{15}Cl_3$

240.0234

240.0235

205.0547 $C_{10}H_{15}^{35}Cl_2$
171.0748 $C_{10}H_{14}^{37}Cl$
169.0778 $C_{10}H_{14}^{35}Cl$
155.0622 $C_9H_{12}^{35}Cl$
133.1012 $C_{10}H_{13}$
127.0309 $C_7H_8^{35}Cl$
105.0700 C_8H_9
89.0153 $C_4H_6^{35}Cl$





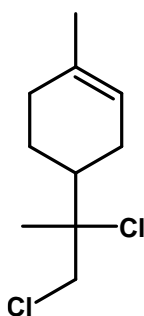
2

22.94 C₁₀H₁₆Cl₂

206.0624

206.0621

171.0932	C ₁₀ H ₁₆ ³⁵ Cl
170.0855	C ₁₀ H ₁₅ ³⁵ Cl
135.1167	C ₁₀ H ₁₅
119.0855	C ₉ H ₁₁
107.0855	C ₈ H ₁₁
93.0699	C ₇ H ₉
91.0542	C ₇ H ₇
79.0542	C ₆ H ₇



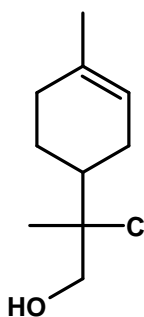
5

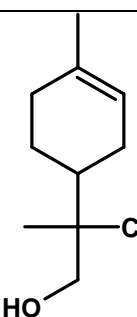
23.56 C₁₀H₁₇OCl

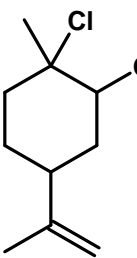
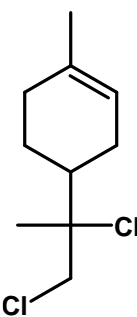
188.0962

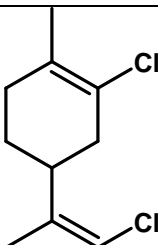
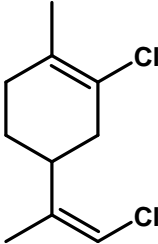
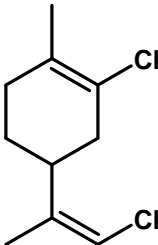
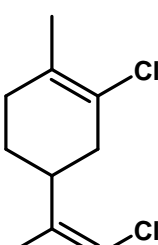
188.0962

173.0726	C ₉ H ₁₄ O ³⁵ Cl
153.1272	C ₁₀ H ₁₇ O
137.0960	C ₉ H ₁₃ O
111.0804	C ₇ H ₁₁ O
93.0698	C ₇ H ₉
83.0491	C ₅ H ₇ O



5		23.63	$C_{10}H_{17}OCl$	188.0962	188.0961	173.0726 171.0570 153.1272 137.0960 111.0804 93.0698	$C_9H_{14}O^{35}Cl$ $C_9H_{12}O^{35}Cl$ $C_{10}H_{17}O$ $C_9H_{13}O$ $C_7H_{11}O$ C_7H_9
---	---	-------	-------------------	----------	----------	---	---

2		24.27	$C_{10}H_{16}Cl_2$	206.0624	206.0622	171.0932 135.1167 107.0854 93.0698 91.0542 79.0542	$C_{10}H_{16}^{35}Cl$ $C_{10}H_{15}$ C_8H_{11} C_7H_9 C_7H_7 C_6H_7
							

3		24.49	$C_{10}H_{14}Cl_2$	204.0467	204.0462	171.0748 167.0621 153.0464 133.1011 115.0542 105.0699 91.0542 79.0542	$C_{10}H_{14}^{37}Cl$ $C_{10}H_{12}^{35}Cl$ $C_9H_{10}^{35}Cl$ $C_{10}H_{13}$ C_9H_7 C_8H_9 C_7H_7 C_6H_7		
3		24.70	$C_{10}H_{14}Cl_2$	204.0467	204.0465	169.0777 155.0621 133.1011 127.0309 91.0543 79.0542	$C_{10}H_{14}^{35}Cl$ $C_9H_{12}^{35}Cl$ $C_{10}H_{13}$ $C_7H_8^{35}Cl$ C_7H_7 C_6H_7	2 ± 0.5	2 ± 0.5
3		25.10	$C_{10}H_{14}Cl_2$	204.0467	204.0466	169.0777 155.0621 133.111 119.0855 91.0543 79.0542	$C_{10}H_{14}^{35}Cl$ $C_9H_{12}^{35}Cl$ $C_{10}H_{13}$ C_9H_{11} C_7H_7 C_6H_7		
3		25.15	$C_{10}H_{14}Cl_2$	204.0467	204.0466	169.0777 133.1011 127.0308 105.0699 91.0542 79.0542	$C_{10}H_{14}^{35}Cl$ $C_{10}H_{13}$ $C_7H_8^{35}Cl$ C_8H_9 C_7H_7 C_6H_7	21 ± 5.9	26 ± 6.0

¹Number of molecules of chlorinated product per billion air molecules within 80 L chambers

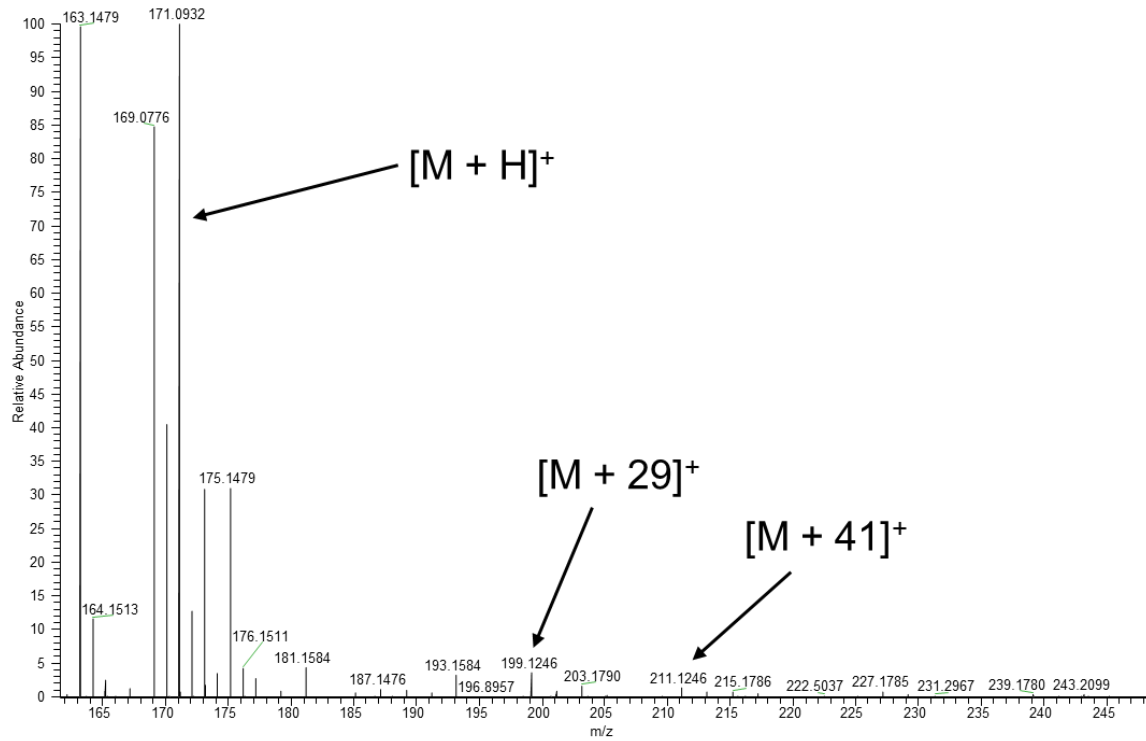


Figure S1. Representative mass spectrum from peak at RT 21.13 min collected in PCI mode, showing the expected adducts and confirming the parent species detected in EI mode, m/z 170.0857 (M^{+*}).

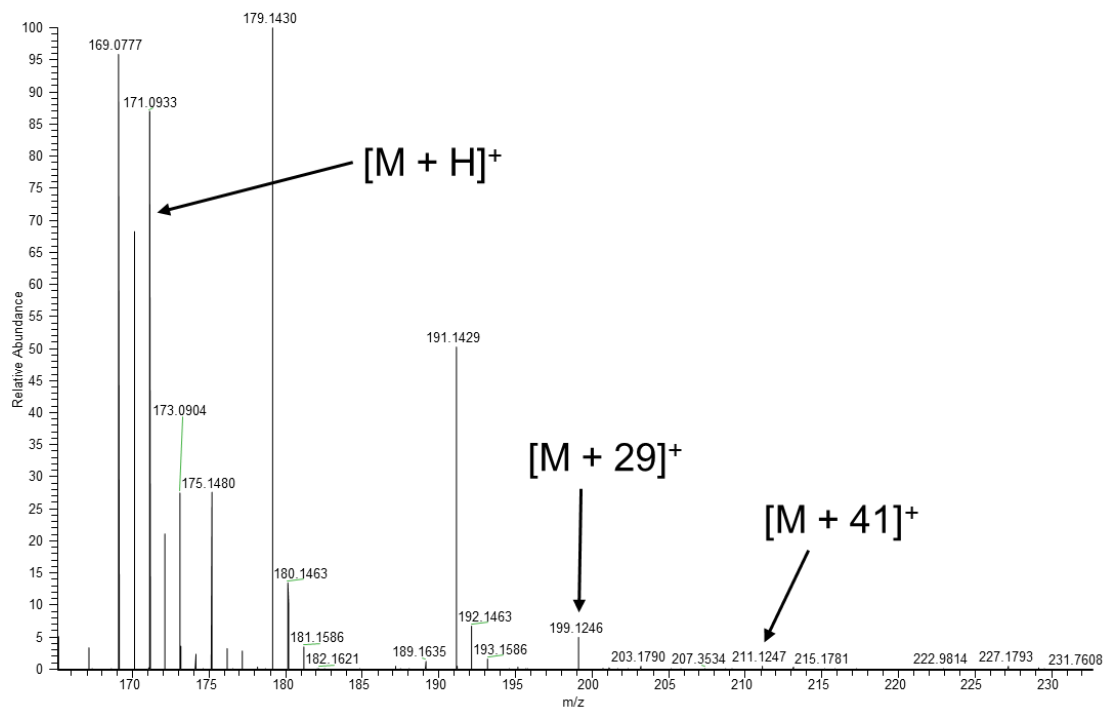


Figure S2. Representative mass spectrum from peak at RT 21.59 min collected in PCI mode, showing the expected adducts and confirming the parent species detected in EI mode, m/z 170.0857 ($M^{+\cdot}$).

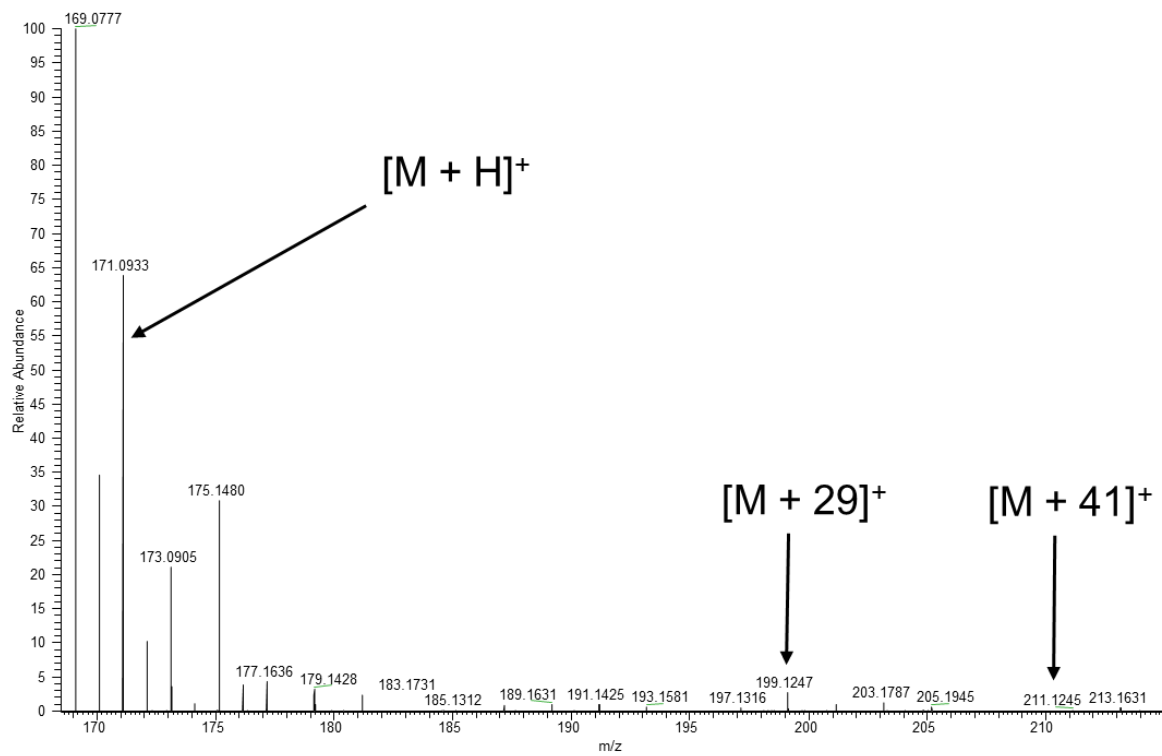


Figure S3. Representative mass spectrum from peak at RT 21.8 min collected in PCI mode, showing the expected adducts and confirming the parent species detected in EI mode, m/z 170.0857 (M^{+*}).

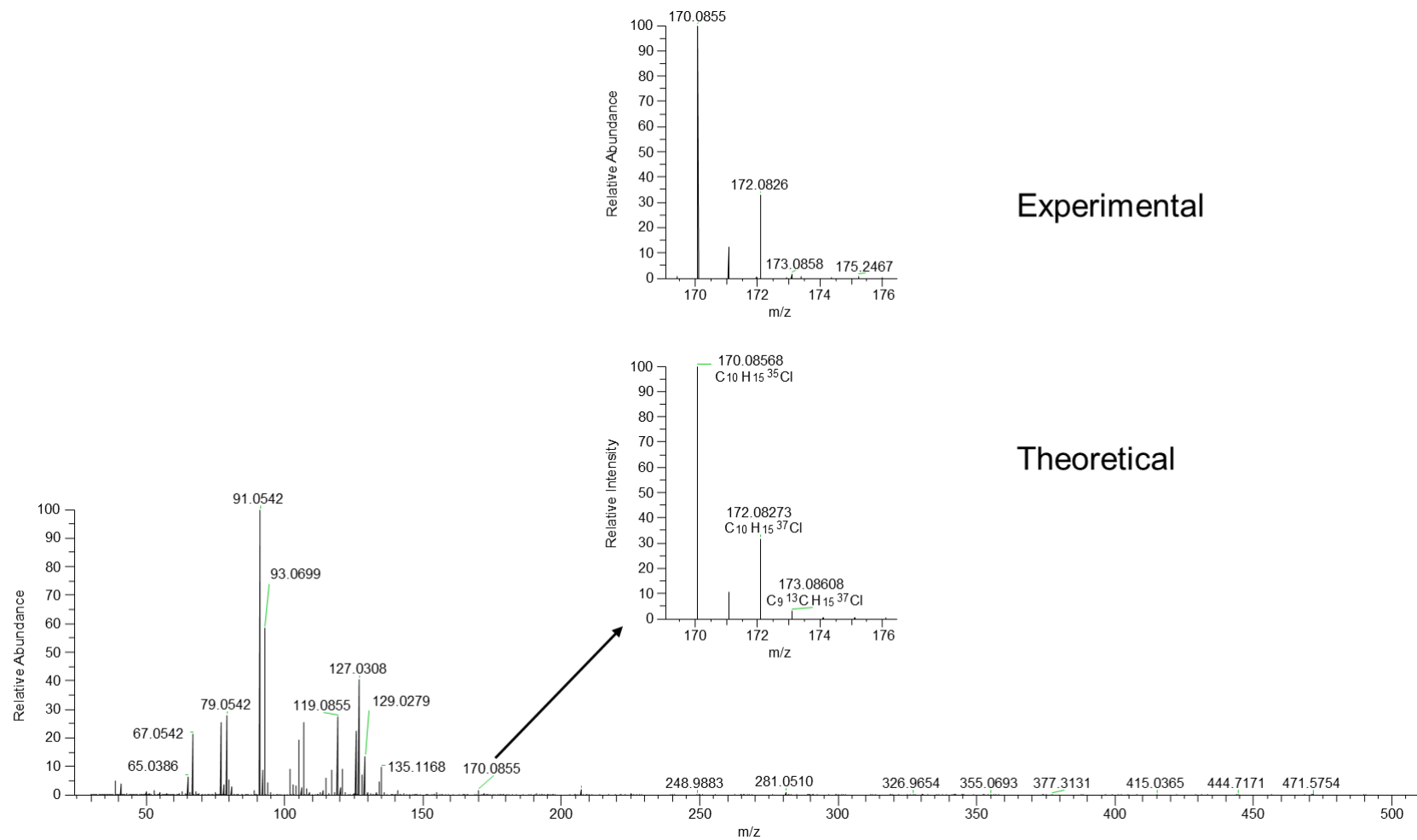


Figure S4. Representative GC-MS chromatogram from singly chlorinated limonene species (1, Table 1) detected at RT 21.13, 21.59, and 21.80 min from the reaction of limonene with HOCl/Cl₂ in the gas phase. The parent ion for this molecule was detected at m/z 170.0855 (EI mode, M⁺), and the inset shows the expected isotopic pattern.

Experimental

Theoretical

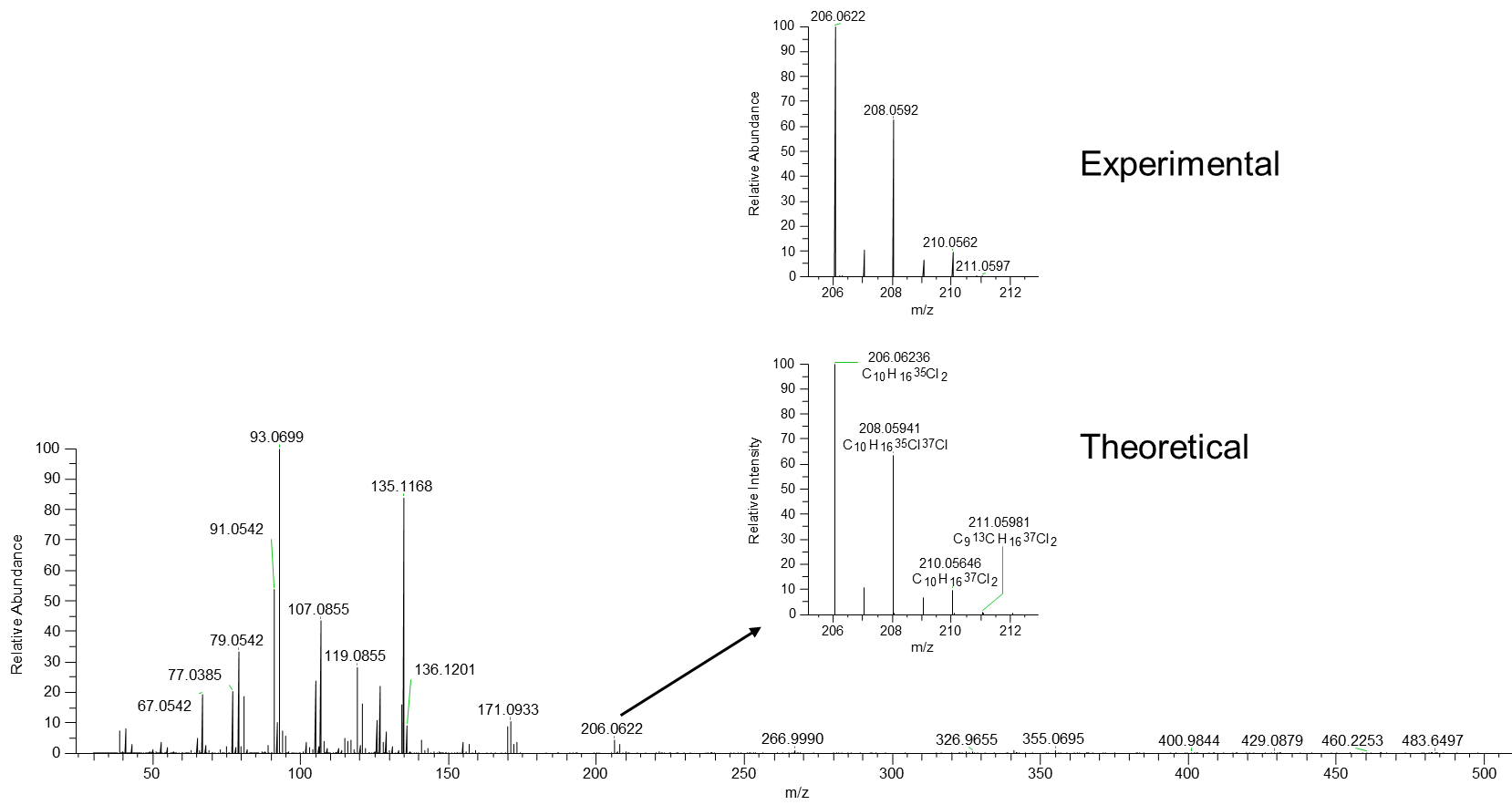


Figure S5. Representative GC-MS chromatogram from dichlorinated limonene species (2, Table 1) detected at RT 22.94 and 24.27 min from the reaction of limonene with HOCl/Cl₂ in the gas phase. The parent ion for this molecule was detected at m/z 206.0622 (EI mode, M⁺), and the inset shows the expected isotopic pattern.

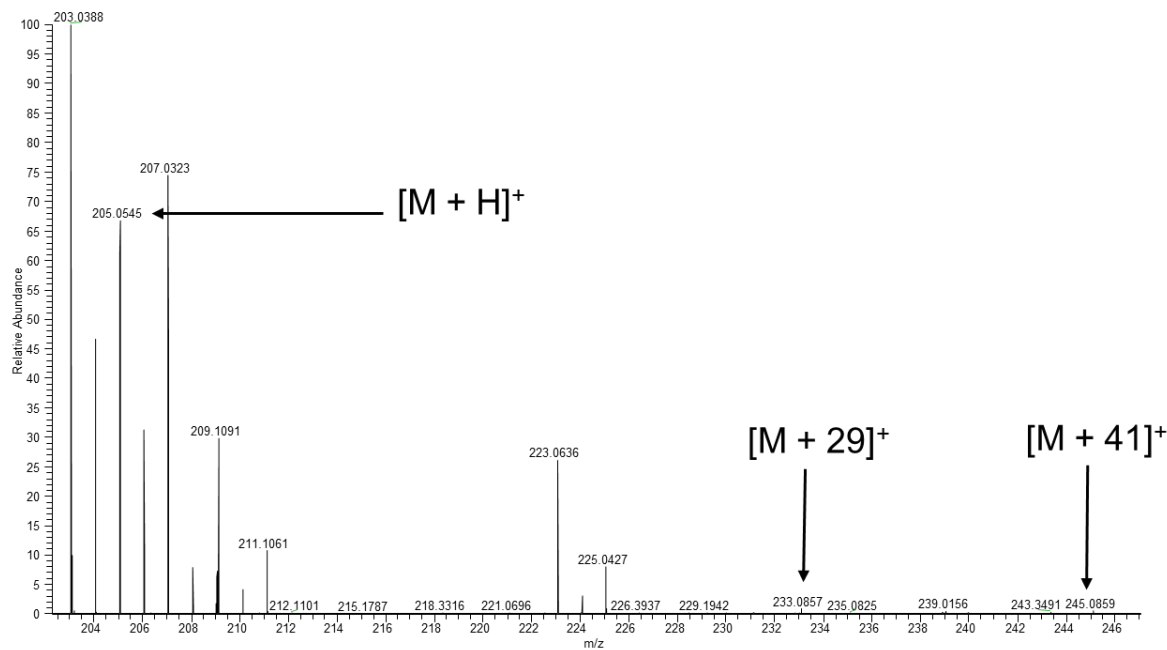


Figure S6. Representative mass spectrum from peak at RT 24.70 min collected in PCl mode, showing the expected adducts and confirming the parent species detected in EI mode, m/z 204.0467 ($M^{+\cdot}$).

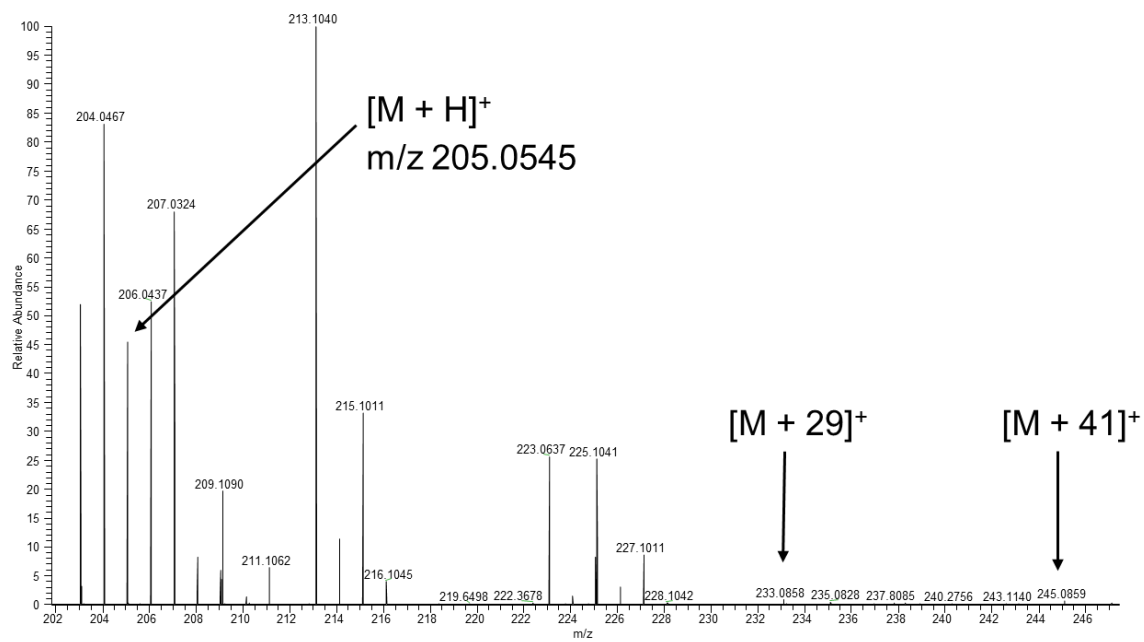


Figure S7. Representative mass spectrum from peak at RT 25.10 min collected in PCI mode, showing the expected adducts and confirming the parent species detected in EI mode, m/z 204.0467 ($M^{+\cdot}$).

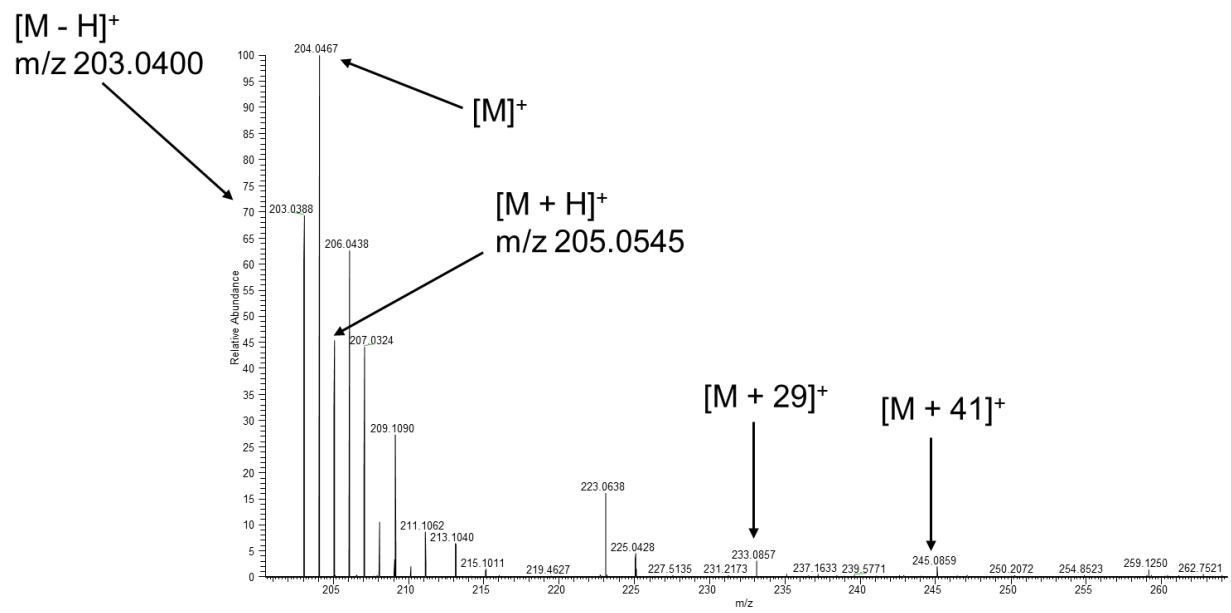


Figure S8. Representative mass spectrum from peak at RT 25.15 min collected in PCI mode, showing the expected adducts and confirming the parent species detected in EI mode, m/z 204.0467 ($M^{+\cdot}$).

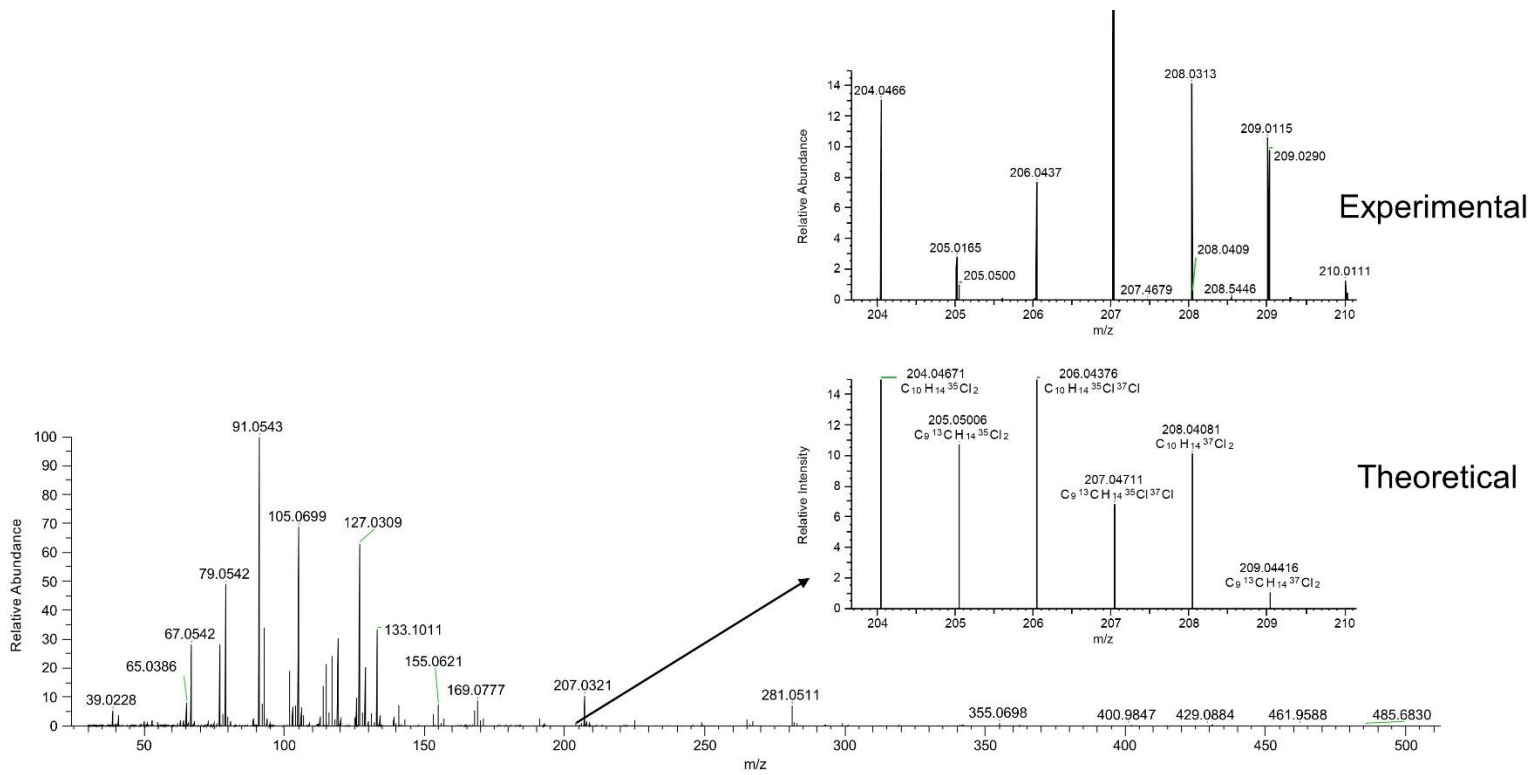


Figure S9. Representative GC-MS chromatogram from dichlorinated limonene species (3, Table 1) detected at 24.49, 24.70, 25.10, and 25.12 min from the reaction of limonene with HOCl/Cl₂ in the gas phase. The parent ion for this molecule was detected at m/z 204.0466 (EI mode, M⁺), and the inset shows the expected isotopic pattern.

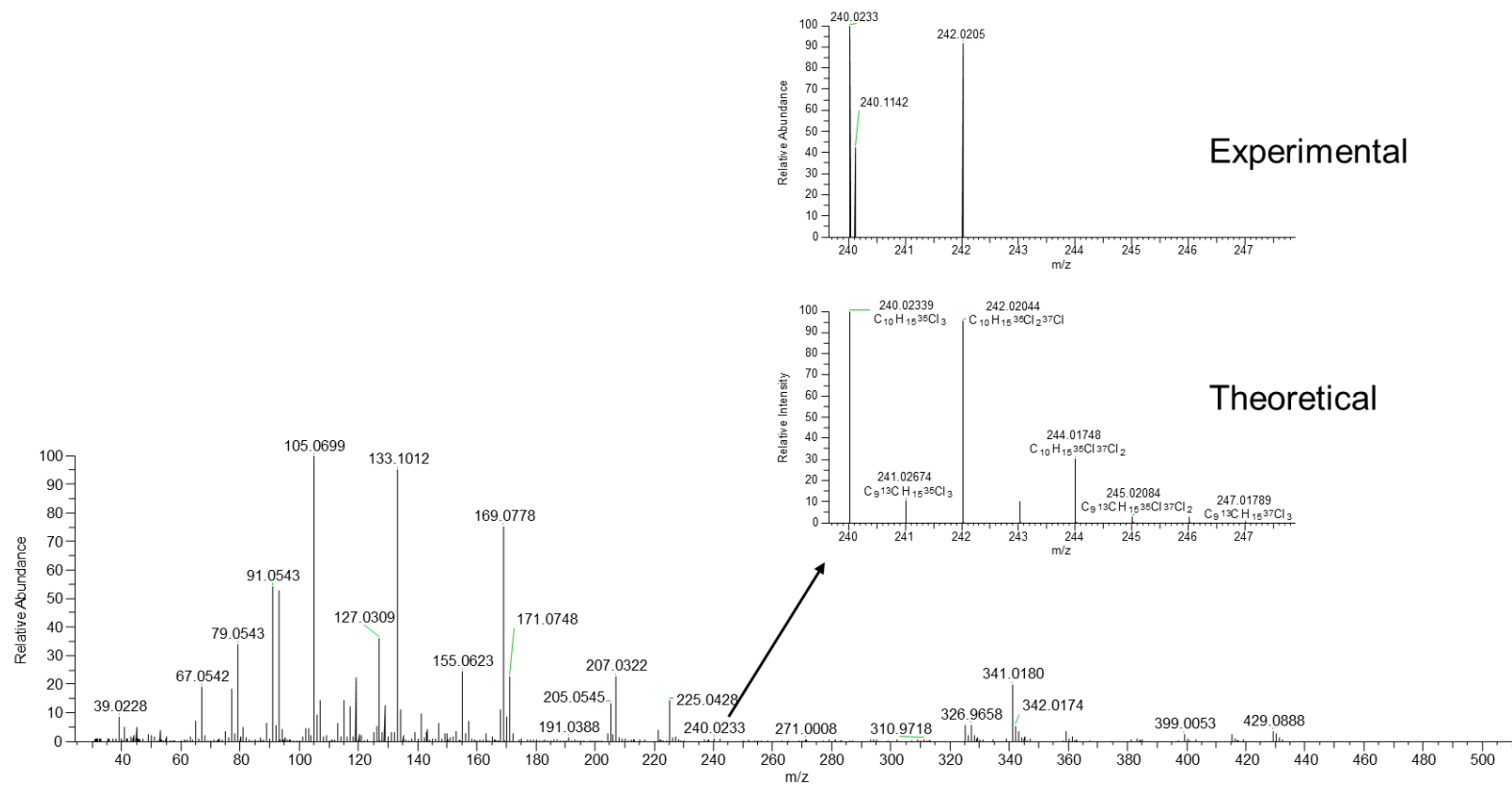


Figure S10. Representative GC-MS chromatogram from tri-chlorinated limonene species (4, Table 1) detected at RT 18.4 and 21.96 min from the reaction of limonene with HOCl/Cl₂ in the gas phase. The parent ion for this molecule was detected at m/z 240.0233 (EI mode, M⁺), and the inset shows detection of the two most abundant isotopes.

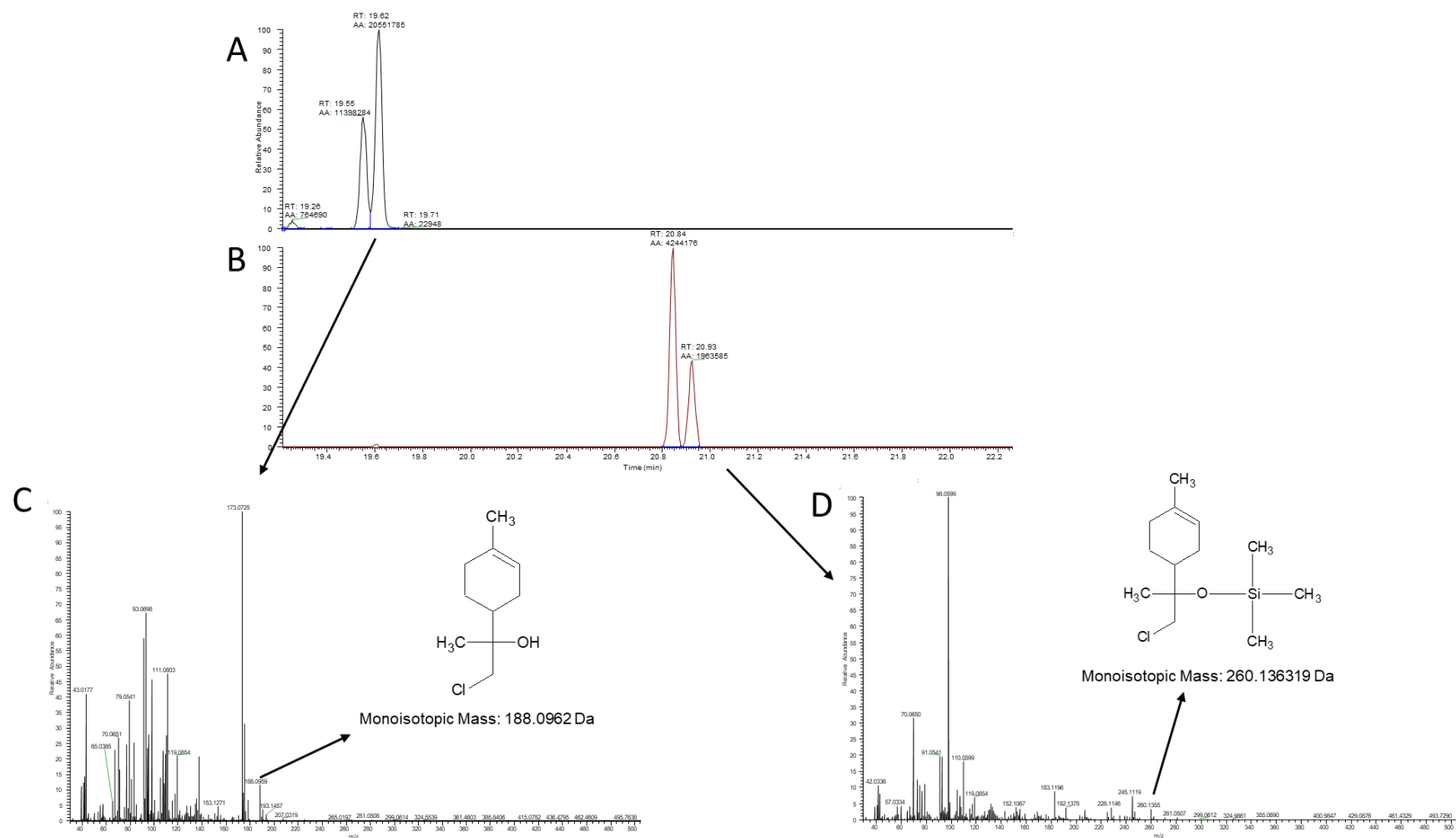
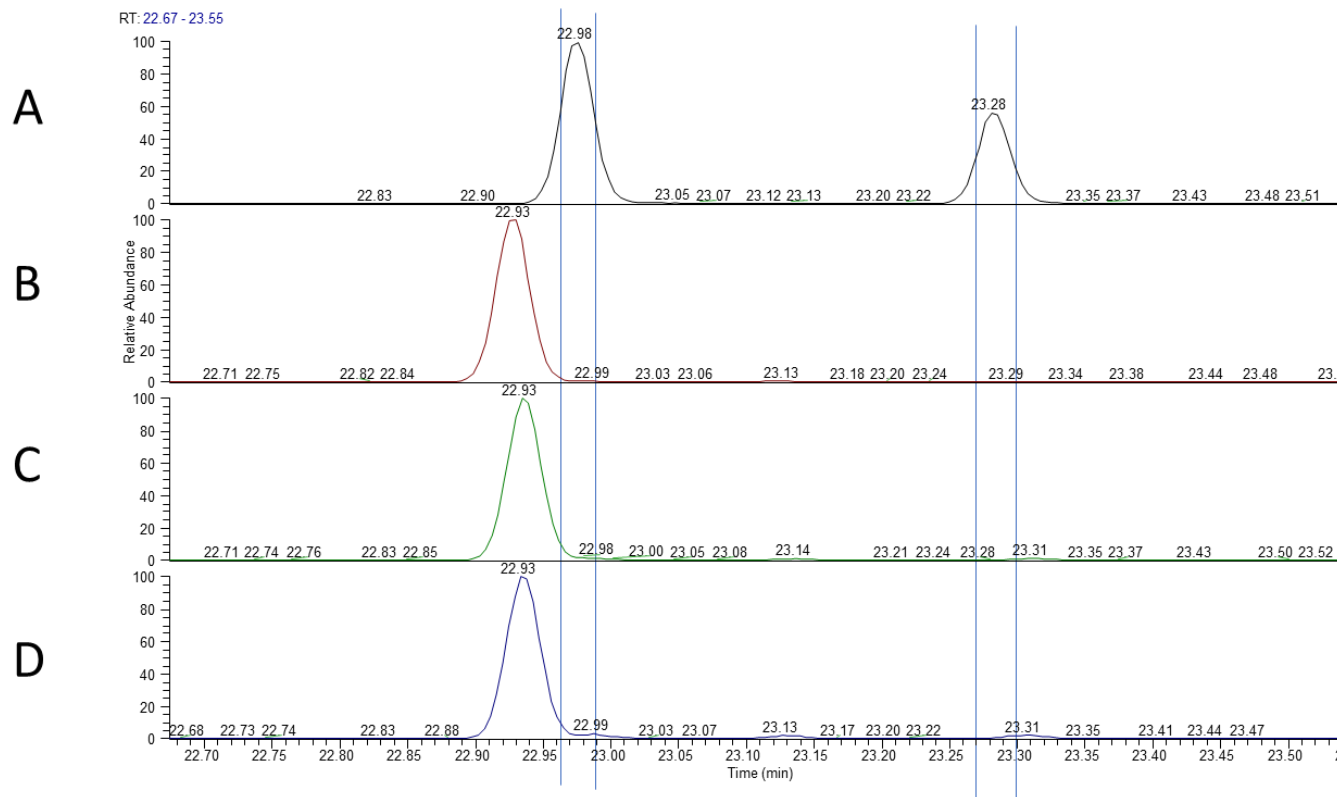


Figure S11. GC-MS extracted ion chromatograms for limonene chlorhydrin (Panel A) and BSTFA-derivatized limonene chlorhydrin (Panel B) and corresponding mass spectra (C and D).



Limonene
chlorohydrin
(endocyclic)

Gas phase
replicate 1

Gas phase
replicate 2

Gas phase
replicate 3

Figure S12. GC-MS extracted ion chromatogram (m/z 135.1171) for synthesized endocyclic limonene chlorohydrin (Panel A) with its two corresponding peaks at RT 22.98 and 23.28 min highlighted with vertical lines. Extracted ion chromatograms (m/z 135.1171) for products generated from the reaction between HOCl/Cl₂ + limonene are shown in panels B-D. As highlighted by the vertical lines, the endocyclic limonene chlorohydrin is not produced at appreciable levels in the gas phase reactions. The peak at RT 22.93 in the gas phase reaction pertains to the dichlorinated limonene (**2**; m/z 206.0625).

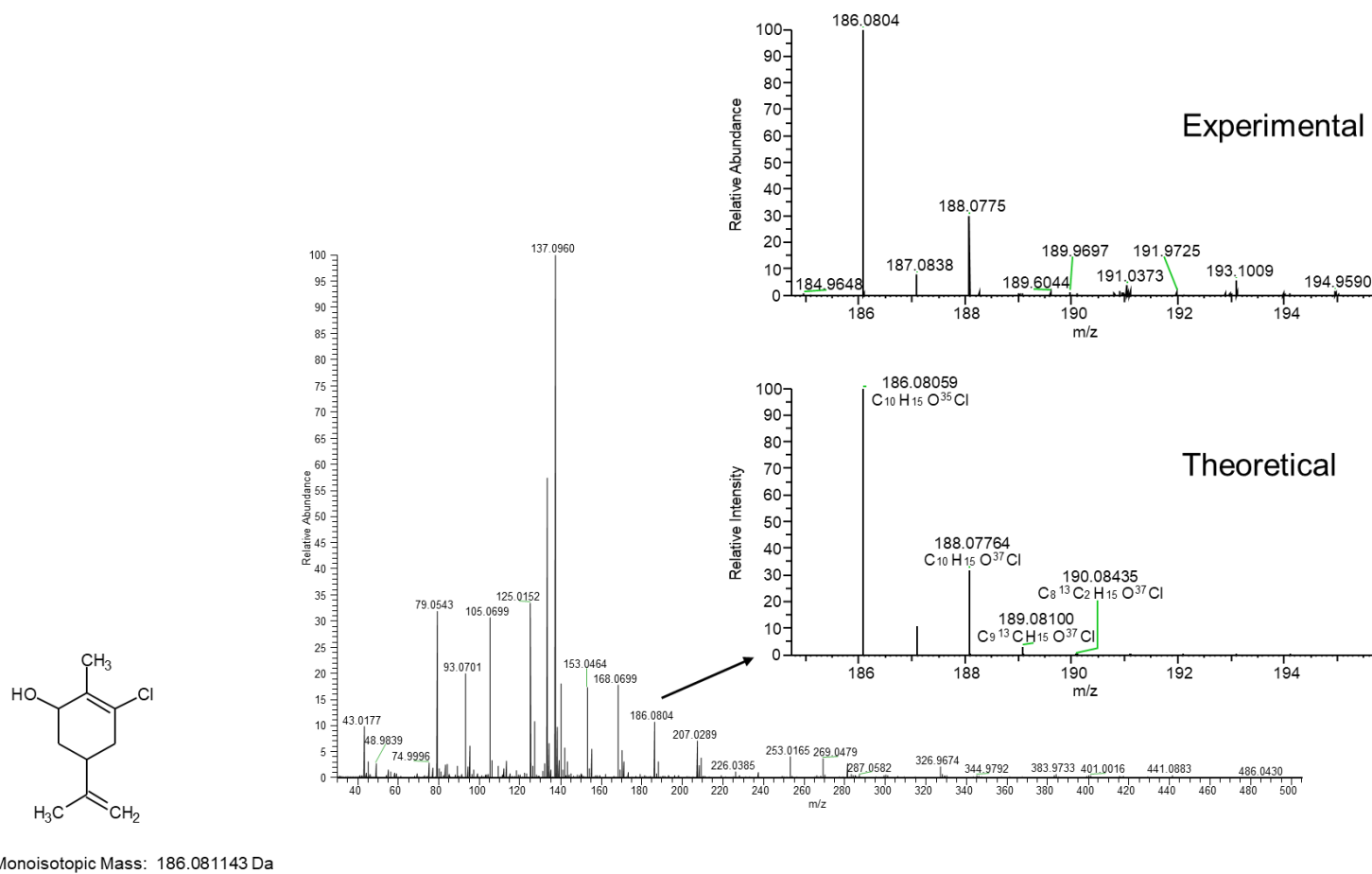


Figure S13. Representative GC-MS chromatogram from chlorinated, oxygenated limonene species detected at RT 22.31 min from the reaction of limonene with HOCl/Cl₂ in the gas phase. The parent ion for this molecule was detected at m/z 186.0804 (EI mode, M⁺·), and the inset shows the expected isotopic pattern.

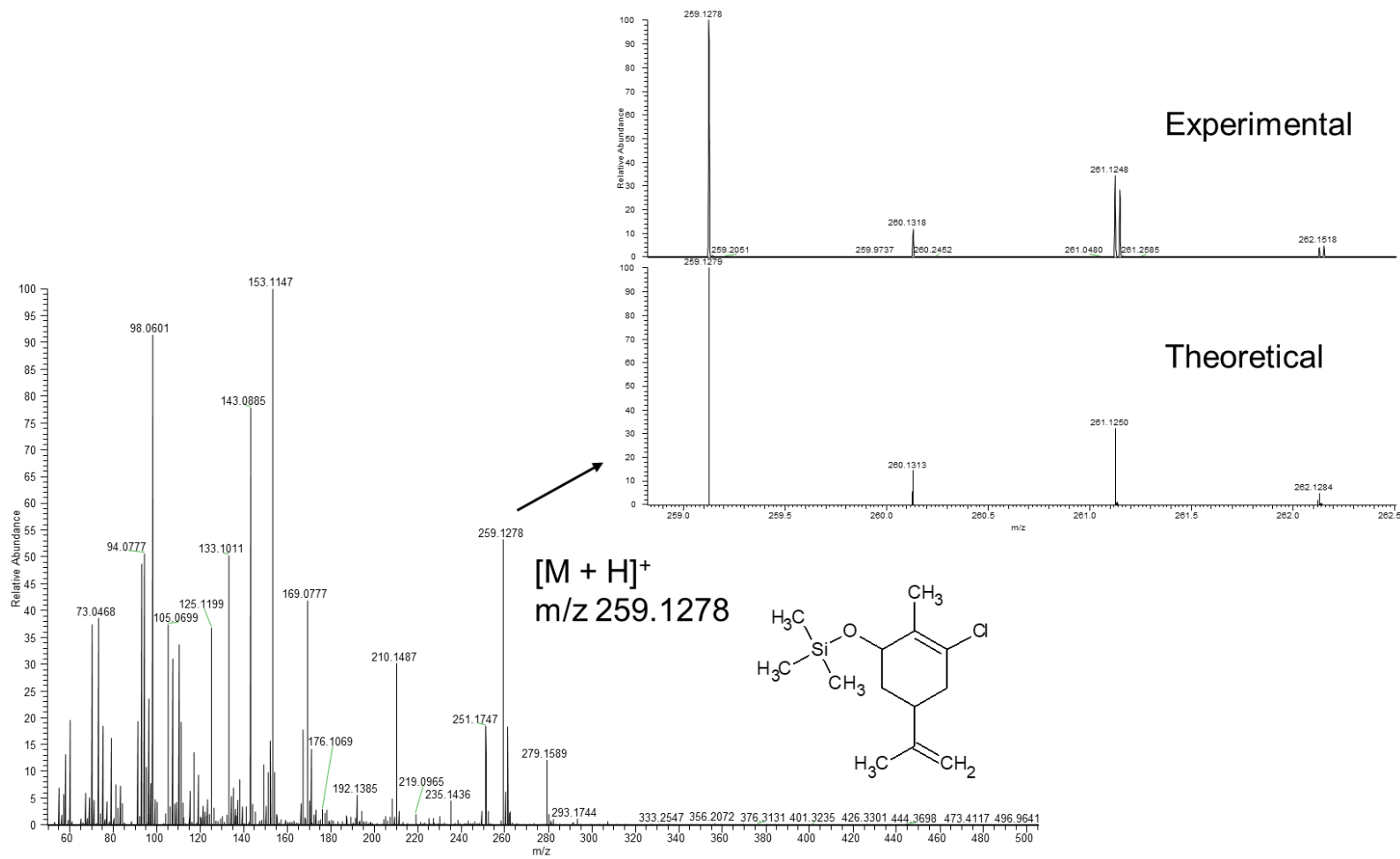


Figure S14. Representative PCI GC-MS spectrum from chlorinated, oxygenated limonene species after derivatization with BSTFA. The species was generated from the reaction of limonene with HOCl/Cl₂ in the gas phase followed by collection by impinger and derivatization by BSTFA. The parent ion for this molecule was detected at m/z 186.0804 (EI mode, $M^{+}\cdot$). The derivatized m/z value 259.1278 $[M + H]^+$ was detected, and the inset shows the expected isotopic pattern.

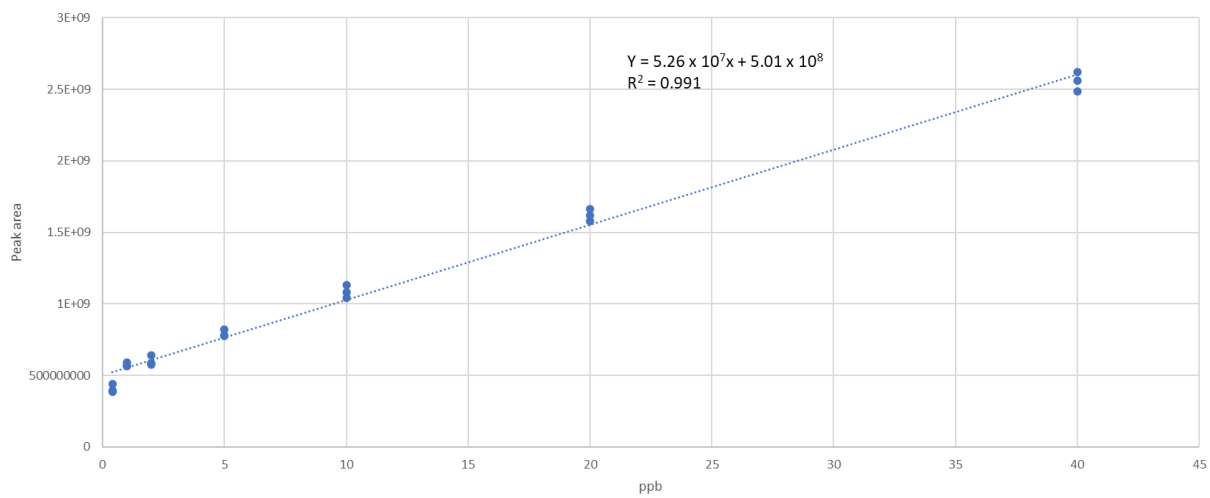


Figure S15. Calibration curve for limonene created from standard canister sampling using a gas preconcentrator with detection by GC-MS. The calibration curve was used to determine concentrations and yields of some chlorinated limonene species.

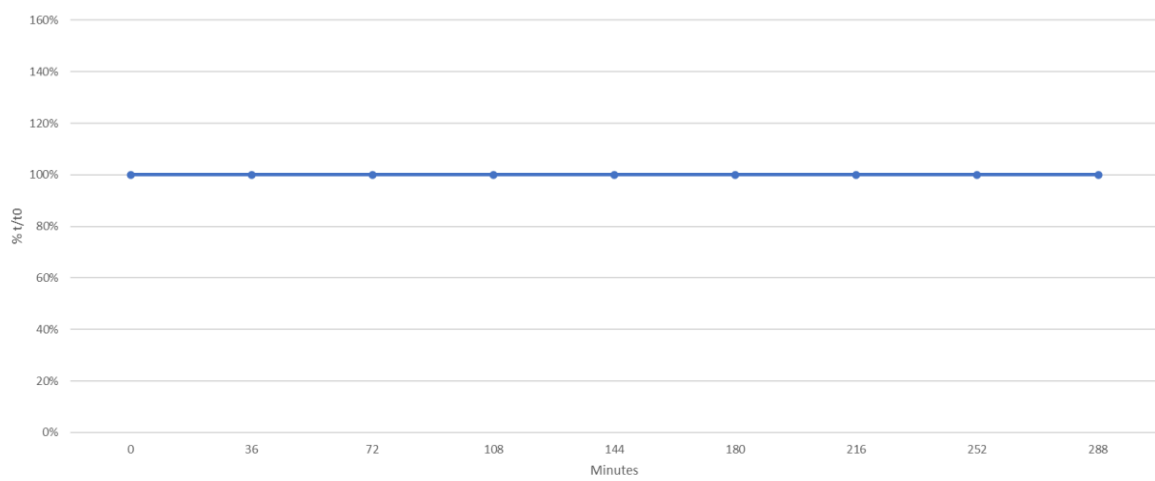


Figure S16. Stability of exocyclic limonene chlorohydrin within a Teflon chamber (50% RH, n=1).

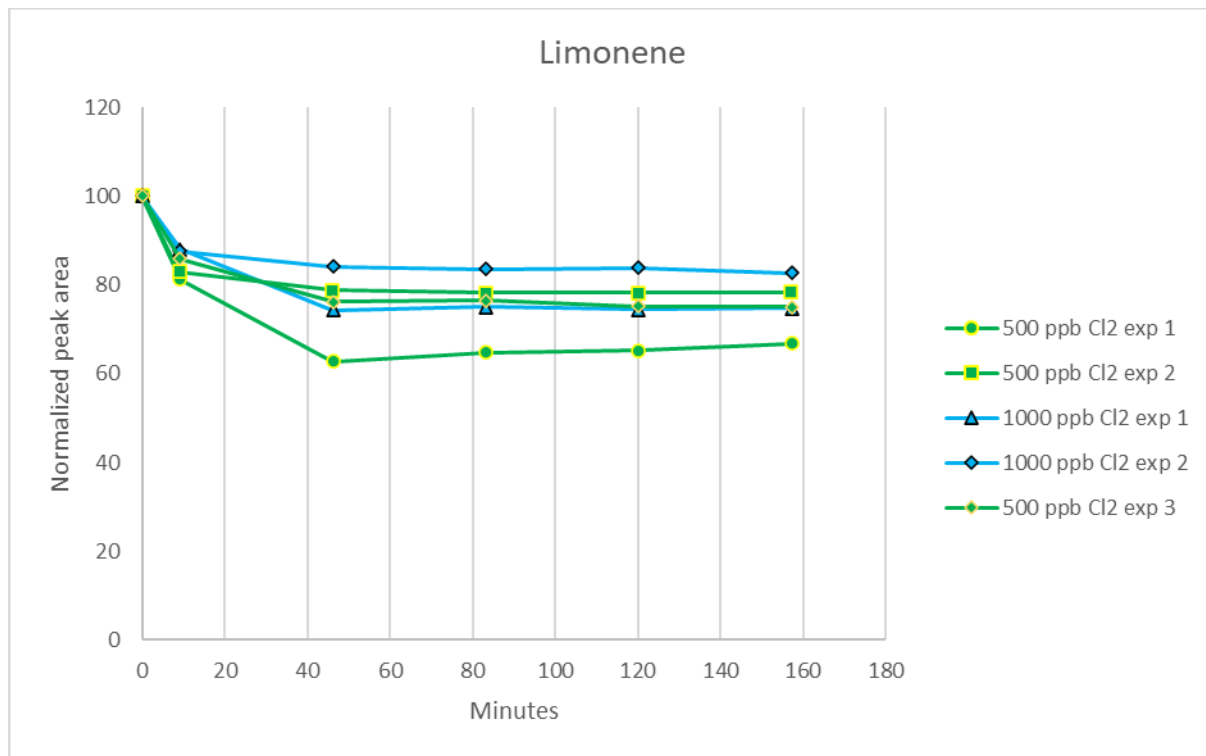


Figure S17. Loss of limonene in several experiments due to treatment with 500 ppb (green traces) and 1000 ppb (blue traces) Cl₂.

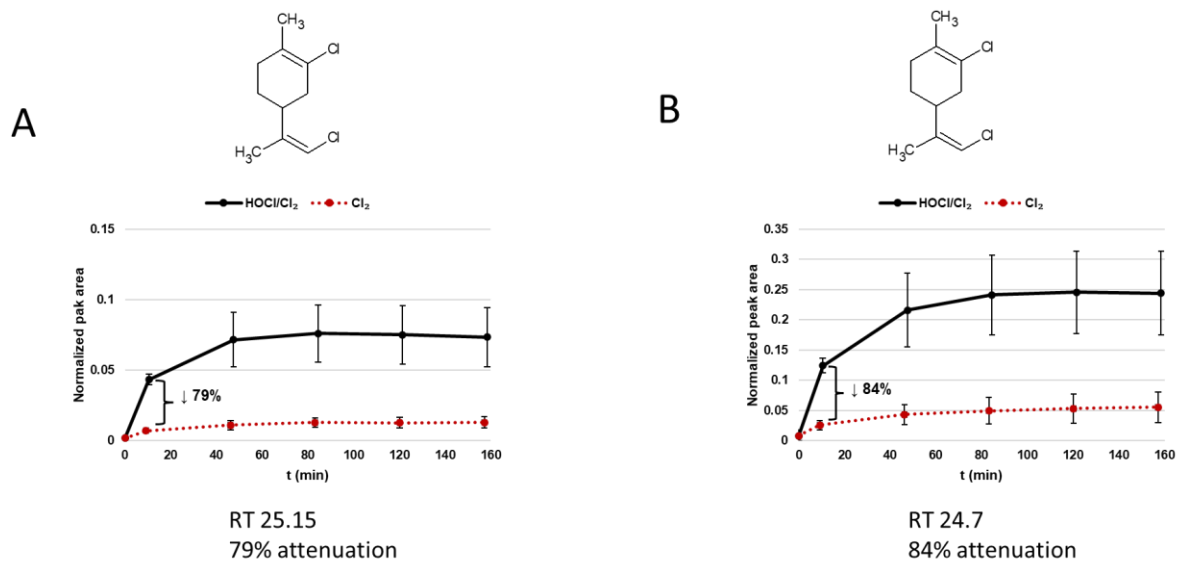


Figure S18. Effect of Cl₂ (red trace) and HOCl/Cl₂ (black trace) on limonene products in gas phase reactions. A) Comparison between effect of Cl₂ and HOCl/Cl₂ on dichlorinated limonene at RT 24.7 min (structure 3 in Table 1). B) Comparison between effect of Cl₂ and HOCl/Cl₂ on dichlorinated limonene at RT 25.15 min (structure 3, Table 1). The normalized peak area pertains to peak area of each species divided by peak area of limonene at time zero. Error bars represent standard deviation with n=3 for limonene + HOCl/Cl₂ and n=7 for limonene + Cl₂.

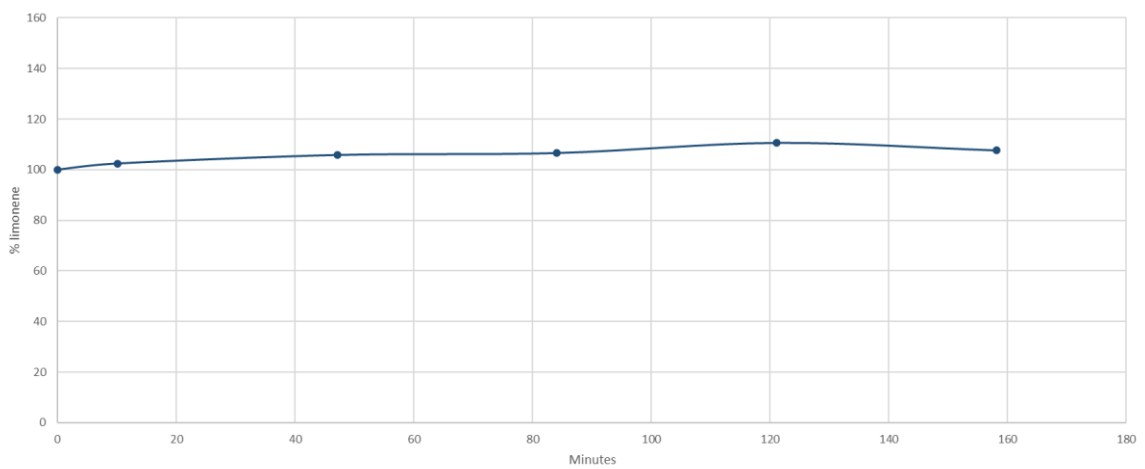


Figure S19. Stability of limonene in low humidity conditions (5% RH, n=1).